Society of Petroleum Engineers

SPE-185548-MS

Dual Porosity Modeling for Shale Gas Wells in the Vaca Muerta Formation

G. J. Manestar and A. Thompson, YPF

This paper was prepared for presentation at the SPE Latin America and Caribbean Petroleum Engineering Conference held in Buenos Aires, Argentina, 18-19 May 2017.

Abstract

The Vaca Muerta shale has been developed for oil and gas production since 2010 and to date nearly 500 wells have been drilled. The large amount of static and dynamic information from these wells has enabled fracture design and production strategy optimization. This paper details the methodology used to integrate all available data in 3D models, in order to understand the impact of rock properties in the production.

The model was simulated using a commercial reservoir simulator, showing that hydraulic fractures are acting as a dual porosity system with a large conductivity (~10 D) connecting a low permeability matrix (~100 nD).

We studied multiple wells in the history match (HM), using separator pressure and choke size as the control variables for the wells, and rates and pressures as comparison variables. A multi-segmented well approach was used to describe the pressure drop inside the well, and a vertical lift performance (VLP) table to describe the flow from the tubing all along to the separator including the wellhead choke.

The static model included the seismic interpretation, stratigraphic framework, geomechanical and petrophysical characterization. Rock permeability, initial pore pressure and total fracture pore volume were calibrated with field measurements used as constraints in the HM process.

Fracture conductivity degradation was introduced in the model to explain observed changes in the wells productivity. Laboratory tests are being designed to validate these hypotheses.

We established early in the project that individual well HM were not unique. It was only through the HM of multiple wells that we were able to reduce the range of uncertainties affecting well performance (matrix permeability, initial water saturation and fracture height). This has given us a more reliable tool to obtain ultimate recovery estimation ranges.

The described model showed a good prediction of a well with water lift problems, giving an accurate forecast for the incremental gas rate after a tubing diameter change. We concluded that the multi-segmented well model is a good representation of the water hold-up fraction behavior.

This methodology enables us to integrate all the knowledge of the subsurface into a model that can be run in short simulation time (~30 minutes), allowing us to iterate quickly during the HM process. The model can be run for single wells or multiple wells and is flexible to adapt for new areas.

We plan to use this methodology to design and monitor pilots in new blocks and to evaluate different development plans for existing projects.

Introduction

The study wells produce from the Vaca Muerta formation in the Nequen Basin, Argentina (Fig. 1). It is composed primarily of intercalations of organic-rich calcareous shales, marls, and micritic limestones, deposited in a distal ramp to basin setting. The proportion and stacking pattern of these facies vary from southeast to northwest, following the geometry of the depositional system (Sagasti et al. 2014). Production fluids are dry gas, gas with condensates or light oil, depending on the source rock maturity (Fig. 1 B).

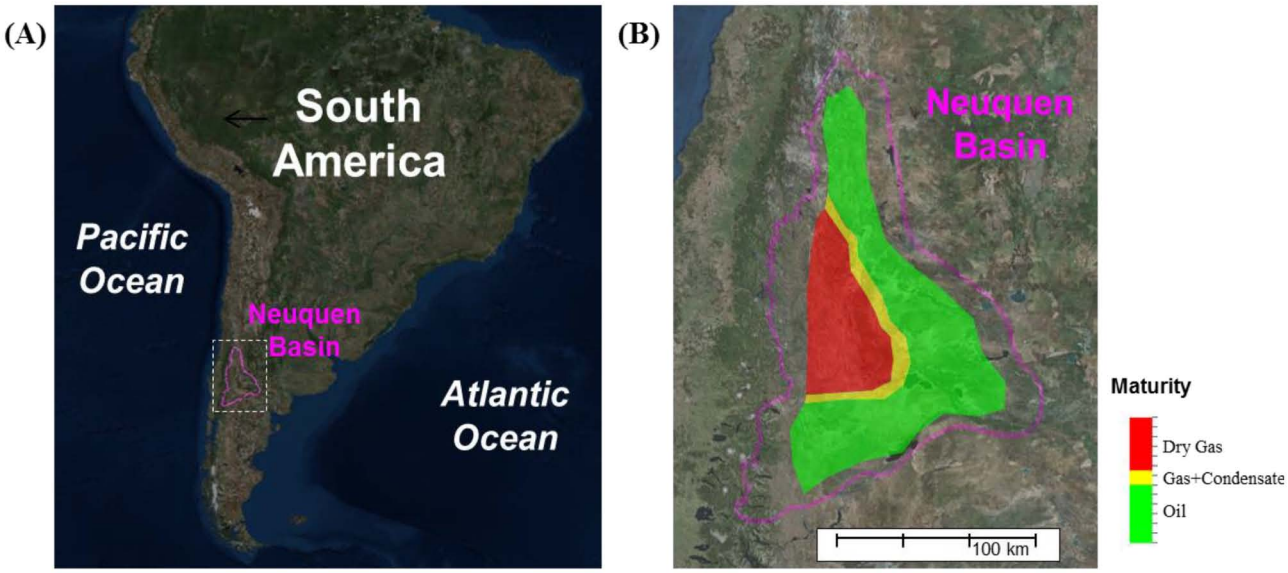

Figure 1—A: Neuquen Basin location. B: Schematic maturity map of the Vaca Muerta shale with different production fluids.

To expand the development to new zones and maximize the profitability of new wells, we needed to study the variations encountered in historical well production to predict sweet spots (geographically and stratigraphically).

Dynamic simulation can help us to understand the impact of the critical parameters that affect the production, with the aim of constraining them for predictions. Non-uniqueness in history match (HM) of this kind of wells has already been studied (Collins et al. 2015). Considering this, our plan is to make multiple forecast cases constraining the parameters by the use of a number wells. It is expected that the HM of multiple using common parameters should reduce the uncertainty existing on them.

Fractured Wells Modelling

As in other unconventional plays, Vaca Muerta wells are stimulated with hydraulic fracture treatments. This treatment interacts with the existing closed natural fractures resulting in a typical complex-fracture-network growth, as evidenced by microseismic monitoring (Weng et al. 2011).

Wells produce from a fractured media confined to a limited stimulated volume around the treated perforations. As the fracture growth is a complex mechanism and measurements methods are indirect, the network extent, geometry and properties are subsequently uncertain.

In wells producing from fractured media, pressure and rate responses can only be represented with the coexistence of two connected flow networks: the rock matrix and the fracture network. This means that we have to choose how to model this secondary pore space representing the fractures, explicitly or implicitly. To solve this issue different approaches have been described in literature with different degrees of complexity:

A. *SRV Modeling:* Consists of the indirect modelling of the hydraulic stimulation as a permeability improvement in a "stimulated rock volume" (SRV) around the perforations and a skin factor. The SRV permeability is a global parameter that includes the combined impact effects of matrix and fractures.
B. *Dual Porosity Modeling:* In this approach both fracture and matrix media are modelled with their own properties considering the finite fractures volume and the conductivity between the matrix and the fractures with a coupling factor. It does not require the actual fracture geometry, only its volume and permeability. However it can include microseismic data to guide the model (Du et al. 2011, Monti et al. 2011).
C. *DFN Modeling:* This uses unstructured gridding with a discrete fracture network (DFN) to explicitly model the flow in the fractures. Fracture geometry can be modelled in detail, using geomechanical simulation that requires elastic rock properties as an input (as the UFM method in Suarez et al. 2015 and Weng et al. 2011). This method models fractures explicitly, though fracture geometry can be scaled up to an equivalent dual porosity model.

A summary table can be seen in Fig. 2.

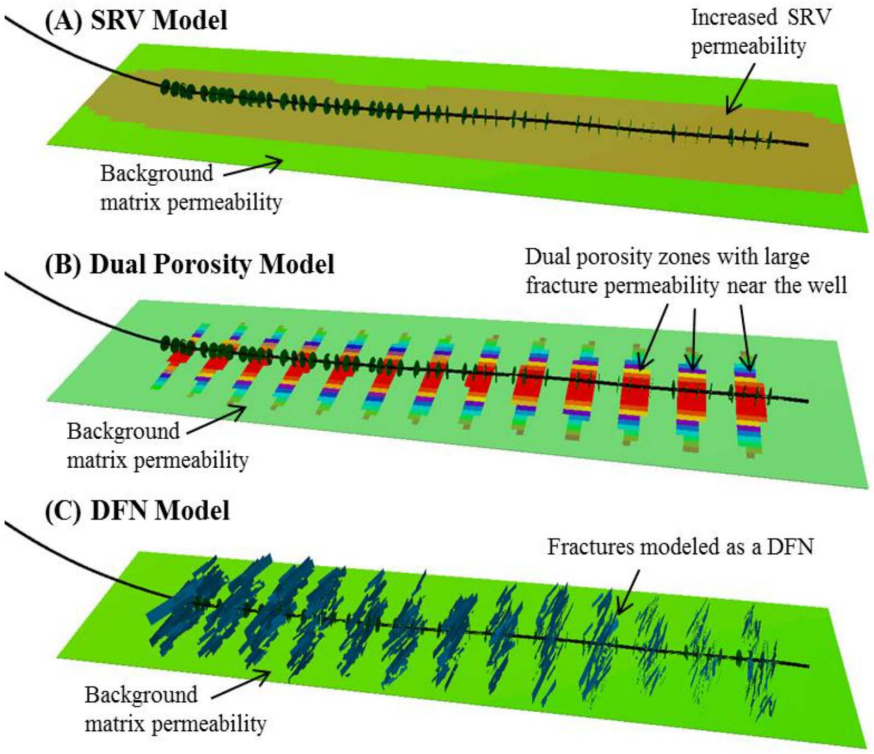

Figure 2—Different ways of model the stimulation effect in well production. A: SRV model as a permeability increased near the wellbore. B: dual porosity model as a secondary system connected to the perforations. C: DFN model representing the hydraulic fractures opened by the stimulation treatment.

We decided not to use the SRV approach (item A) because it is not possible to estimate separately the influence of the rock properties and the completion efficiency. Cipolla et al. (2014) has shown that SRV does not provide any insight into two critical parameters: hydraulic fracture area and conductivity. This reference also suggests that SRV interpretation is poorly linked to the actual fracture geometry and distribution of fracture conductivity.

Using the unstructured gridding to simulate the DFN (item C) is challenging because it requires a determination of the fracture geometry which is a major uncertainty. It can be estimated considering elastic parameters of the rock and using geomechanics software, however calibration is still challenging. This approach is currently being used in YPF to study the effects of well spacing and interference (Suarez

et al. 2017; Suarez et al. 2015) and it can be checked against microseismic data. For the scope of this work -studying the impact of geological variations in the productionthe DFN method would be slower and inefficient.

The dual porosity model selected (item B) in this paper was first described in Vaca Muerta by Monti et al. (2011) for vertical wells. We will show how we apply this model to horizontal wells, how the fracture geometry is related to the model parameters and how well effects (tubing diameter, choke, well length, etc.) can be included to predict productivity changes. The limitations of dual porosity compared to DFN models have been studied by Dershowitz et al. (2000).

Dual Porosity Model Parameters

As developed by Warren and Root (1963) the dual porosity model assumes that fluid in the matrix flows only to the fractures and not to other matrix blocks. The fractures conduct the fluid to neighbor blocks and to the well.

The model introduces a multiplying factor for matrix-fracture flow called *matrix-fracture coupling factor* (also called sigma factor). As we show in Appendix A, this parameter can be related to the fracture spacing (d) as

$$d = \sqrt{12/\sigma}$$

An additional parameter is the fracture porosity (ϕ_f). This is essentially the fractures thickness (e) and the proppant porosity inside the fractures (ϕ_p) referred to the rock bulk volume (see Appendix A) as

$$\phi_f = \phi_p \frac{(d+e)^3 - d^3}{(d+e)^3}$$

The area per volume unit (a_V) is related to sigma (see Appendix A) as

$$a_V \cong \sqrt{3\sigma}$$

With these equations we can correlate the model parameters σ and ϕ_f with geometrical parameters as fracture spacing and aperture (see Fig. 3).

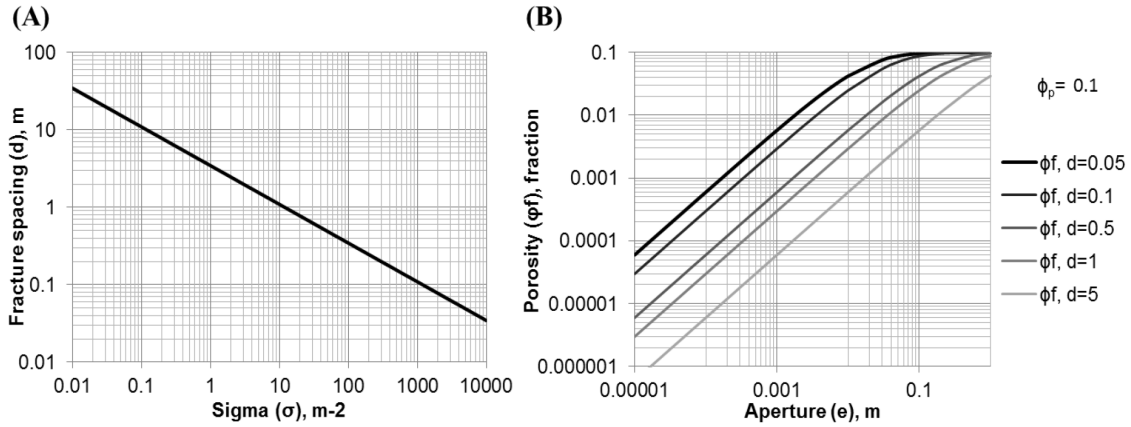

Figure 3—A: Relationship between fracture spacing (d) and matrix-fracture coupling parameter (σ). B: Relationship between fracture porosity (ϕ_f) and fracture aperture (e).

We also need to define the fracture permeability (k_f). This is usually related with the fracture aperture (e) by the equation usually known as *cubic law* (because flow is proportional to the cube of aperture):

$$k_f = \frac{e^2}{12}$$

However, as this correlation is a rough approximation, we use fracture permeability as a HM parameter.

The HM parameters will be porosity, permeability and sigma value for the fractures. We set an individual value of each parameter for each well, considering a distance weighting law that degrades the fracture properties moving away from the well perforations/fracturing points (as this quality reduction with distance is described in the literature, for example Fuentes et al. 2015). This assumption allows us to reduce the amount of parameters of the problem without simplifying the physics of it.

However, we have scaled up different DFNs to dual porosity models with the Oda algorithm (Oda 1985; Dershowitz et al. 2000) and corroborated the relationships described above (see Fig. 4). This way we could get an equivalent DFN that matches the parameters obtained in HM.

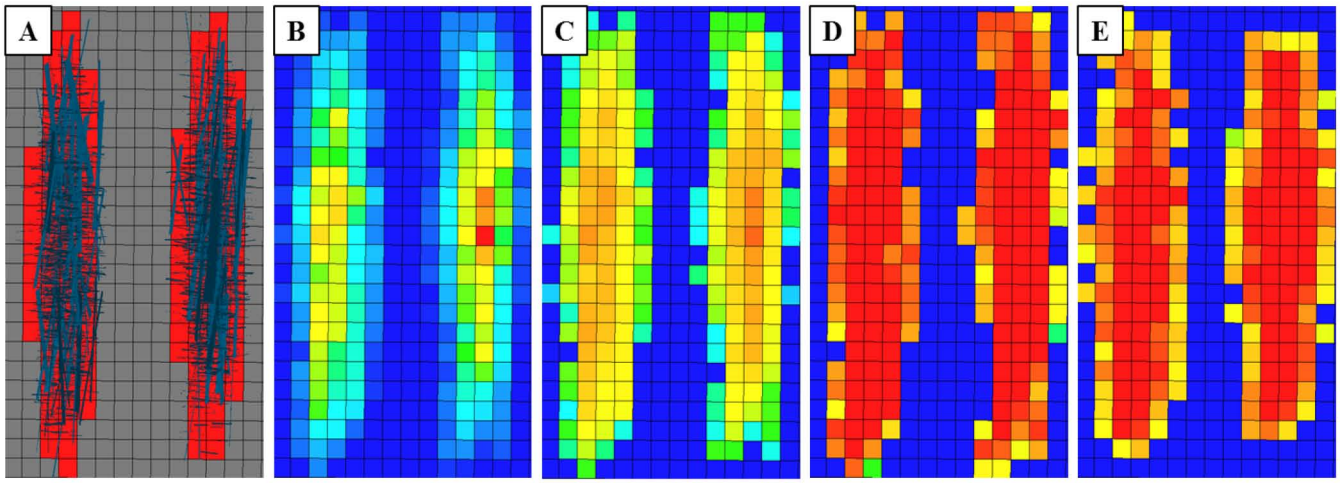

Figure 4—Properties of the dual porosity model scaled up from the DFN. A: Planes of the DFN with active fracture cells in red in the background (used to constrain the DFN). B: Porosity. C: Sigma value. D: X-permeability. E: Y-permeability.

As a final consideration we use the fracture size and porosity assuming that total fracture pore volume should be cross referenced against the total amount of injected treatment fluid. The fracture pore volume should always be less than the injected fluid volume.

Well Control

We chose to simulate the wells controlling them by its separator pressure and the choke diameter, which are fixed and reliable values. Gas rate, water rate and bottom-hole pressure (BHP) are predicted and compared to historical data. Since these parameters frequently have measurement errors, using them as comparison rather than controlling parameters makes the model more predictive and also enables us to simulate different production regimes.

To obtain the BHP data from tubing head pressure (THP) measurements we used multiphase flow calculation software that uses the Gray correlation (Gray 1974) to calculate a pressure profile along the well under different gas rates, water-gas ratio (WGR) and condensate-gas ratio (CGR).

As choke diameter is an input to our model, we calibrated it using the pressure drop and the rates across the wellhead. Gas production is sensitive to choke diameters, specifically at low diameters, so this calculation let us use a more reliable choke history. We have use the Perkins correlation (Perkins 1993) to calculate the "effective choke size diameter" that is acting in the wellhead using the pressures before and after the choke and the flow rates at control points. Then calculated choke diameter is a function of gas rate (q_g), WGR, CGR, THP (p_{wh}) and line pressure (p_l):

$$D_{ch} = f\left(q_g, \text{WGR}, \text{CGR}, p_{wh}, p_l\right)$$

This brings some differences with historical choke diameters that have been included in the simulator, as shown in Fig. 5.

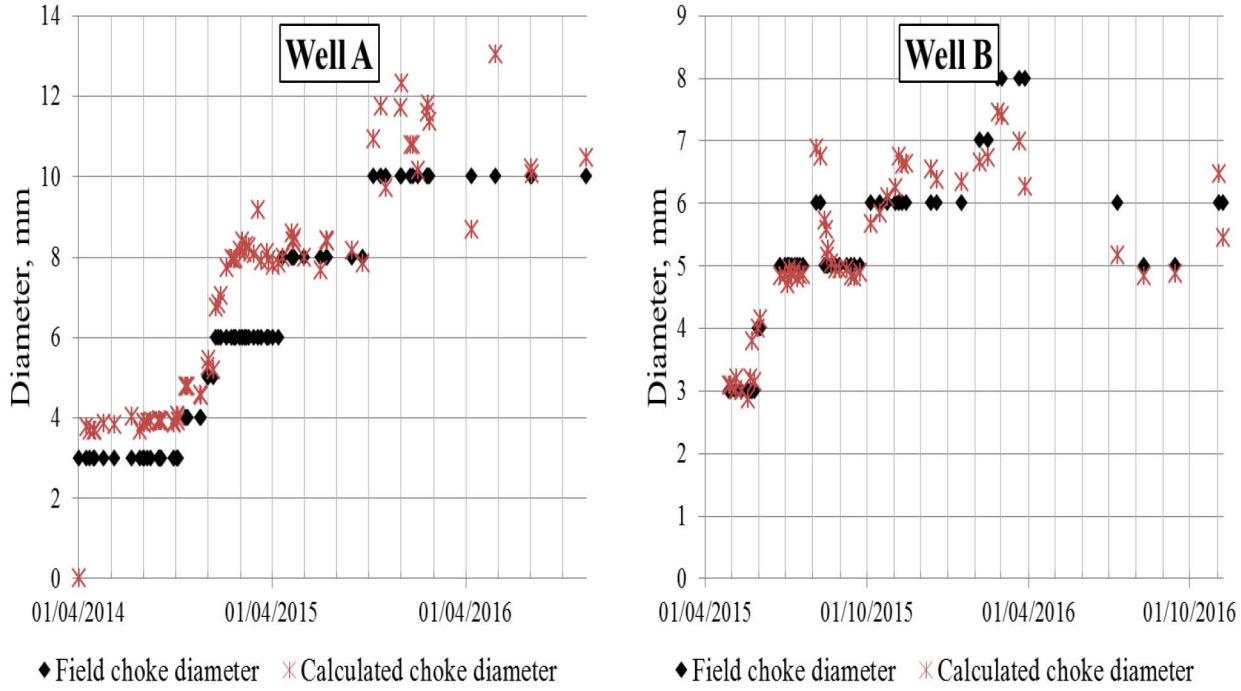

Figure 5—Calculated diameter using the pressure drop in the choke in two sample wells, showing some differences.

The pressure drop from the reservoir to the wellbore is calculated using the Russell-Goodrich dry gas pseudo-pressure equations that alter the free gas mobility to account for its pressure dependence between the grid block pressure and the connection pressure (Russel et al. 1966).

For the calculation of the pressures along the well to the separator pressure we divided the well into two sections in the simulator using two methodologies (see Fig. 6):

1. The first section encompasses from the well bottom to the beginning of the tubing (the BHP datum depth) through the horizontal interval. This is modeled dynamically using the multi-segmented wells model. This method assumes that the wellbore can be divided into a number of segments (Holmes et al. 1998). This enables us to simulate the fluid distribution changes inside the casing through time including the acceleration and friction components of pressure drop along the long horizontal well path.
2. The pressure drop from the BHP datum through the tubing, the choke and to the separator is simulated using a vertical flow performance (VFP) table. This table relates the separator pressure with the gas rate, water-gas ratio, oil-gas ratio, choke size and bottom-hole pressure (standard procedure). This VFP table was constructed with specialized software using the Gray correlation that is suitable for dry gas (or low condensate gas) in the vertical section, the Perkins correlation in the choke, and the Beggs and Brill correlation (Beggs et al. 1973) for the surface horizontal lines.

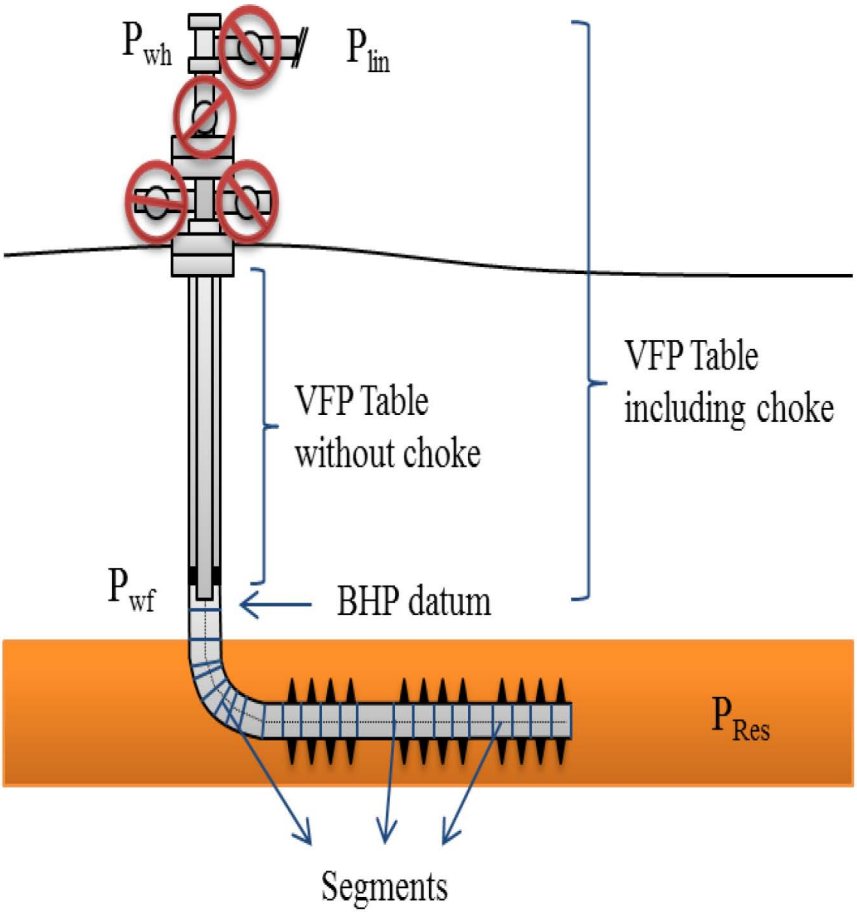

Figure 6—Schematic picture of a well showing the different methodologies used for pressure drop calculation. The segments that divided the bottom section of the well for the calculations are marked in blue. In the vertical tubing section, two different VFP tables were constructed including or not the pressure drop across the choke.

We assume we can use the VFP table in the tubing because liquid holdup problems are more likely to occur in the casing section where there is a larger cross section area and lower fluid velocity. Then the BHP value at the bottom of the tubing can be calculated with the THP value using the VFP table without considering dynamic effects as we need to do in the horizontal part.

The segmentation of the wellbore allows us to simulate the well effects that usually distort the reservoir effects. This was critical because differences in water-gas ratios have a large impact on well productivity.

We tested this model using historical data before and after the installation of a "velocity string" in a well. A velocity string is a reduced diameter piece of tubing in the bottom of the well that increases the fluid velocity to reduce the effect of liquid holdup. Some wells showed this problem and achieved up to a 25% production increment after installation of a velocity string. This change was caused by liquid accumulation in the wellbore, so it was impossible to represent the productivity change without a multi-segmented well model. Fig 7 shows a well HM and the liquid holdup prediction through the well in the segments in the model, showing the expected behavior.

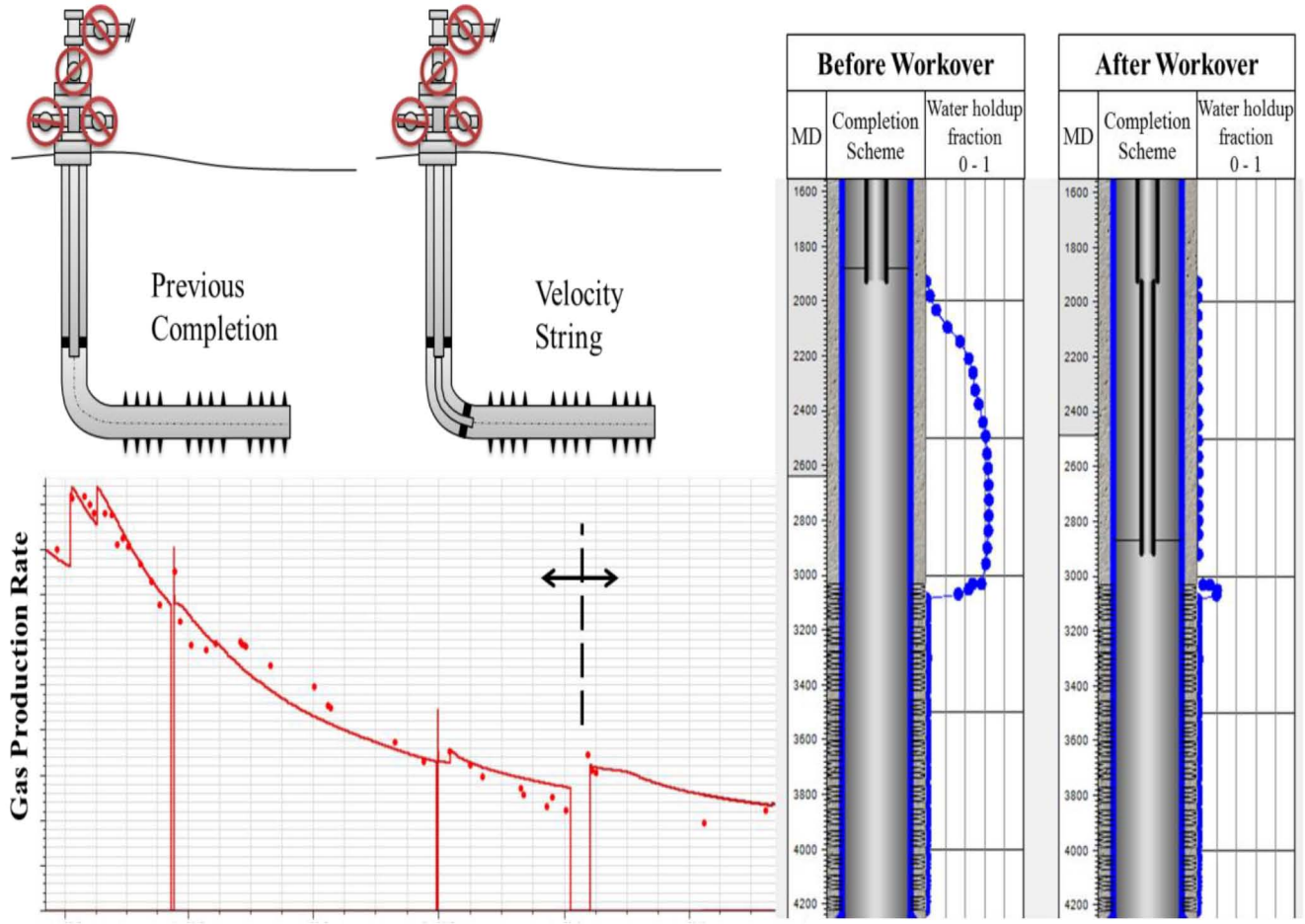

Figure 7—Scheme of the production string before and after the installation of the velocity string in the well, the increase in gas production rate and the change in the water holdup fraction profile along the segments.

Static Model

A full field static model was built by the geoscientists based on the reservoir characterization, including porosity, permeability and water saturation constrained with a facies distribution.

This large model (10 km average length) includes several wells and cannot be simulated because of computational limitations. Since well interference is not expected over large distances, full field simulation is not required.

To simulate these wells, a fine resolution grid is required, because large pressure gradients need to be represented showing the pressure change moving from the induced fractures into the tight matrix. The size of the static model should include a number of wells that could potentially interfere with each other. However simulation often reveals that single well models are adequate.

Cell size is potentially a key variable so we evaluate what is a good compromise between areal cell size and potential numerical dispersion.

Below we show simulated two-well sector model in 1500 m length horizontal wells that are in similar locations but navigating different stratigraphic intervals (Fig. 8).

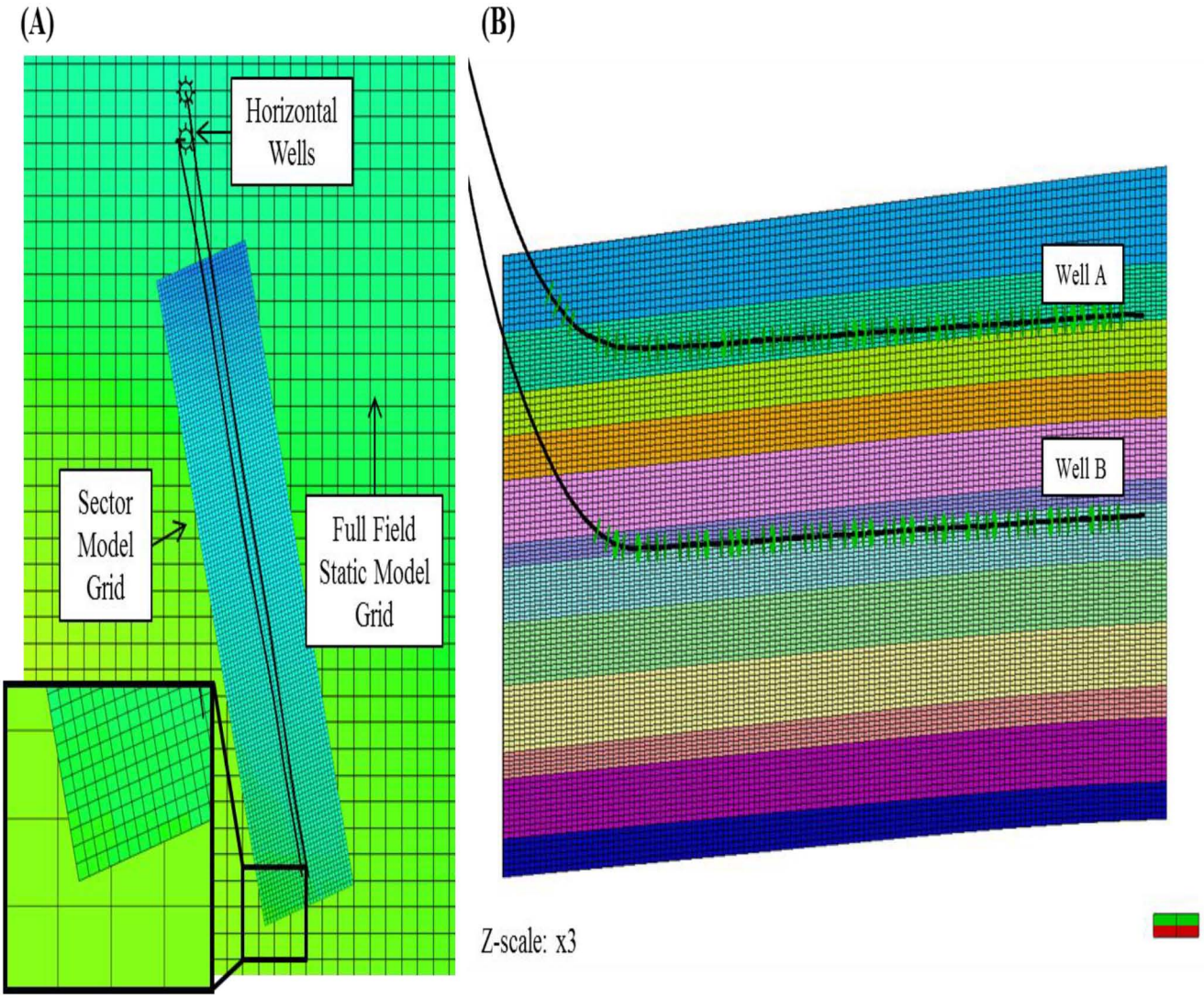

Figure 8—A: Sector model (10 m cell size) and portion of the full field static model (50 m cell size) showing the scale change for simulation requirements. B: Cross section of the model showing the sector model used for the simultaneous simulation of two wells in the same location navigating two different stratigraphic levels.

We tested different cell sizes (see Fig. 9):

- 10 meters. 0.4 million cells. Runtime: 11 minutes.
- 5 meters. 1.6 million cells. Runtime: 62 minutes.
- 2.5 meters. 6.5 million cells. Runtime: 6 hours.

The difference in the simulation results was less than 5%, enabling us to select the fastest model.

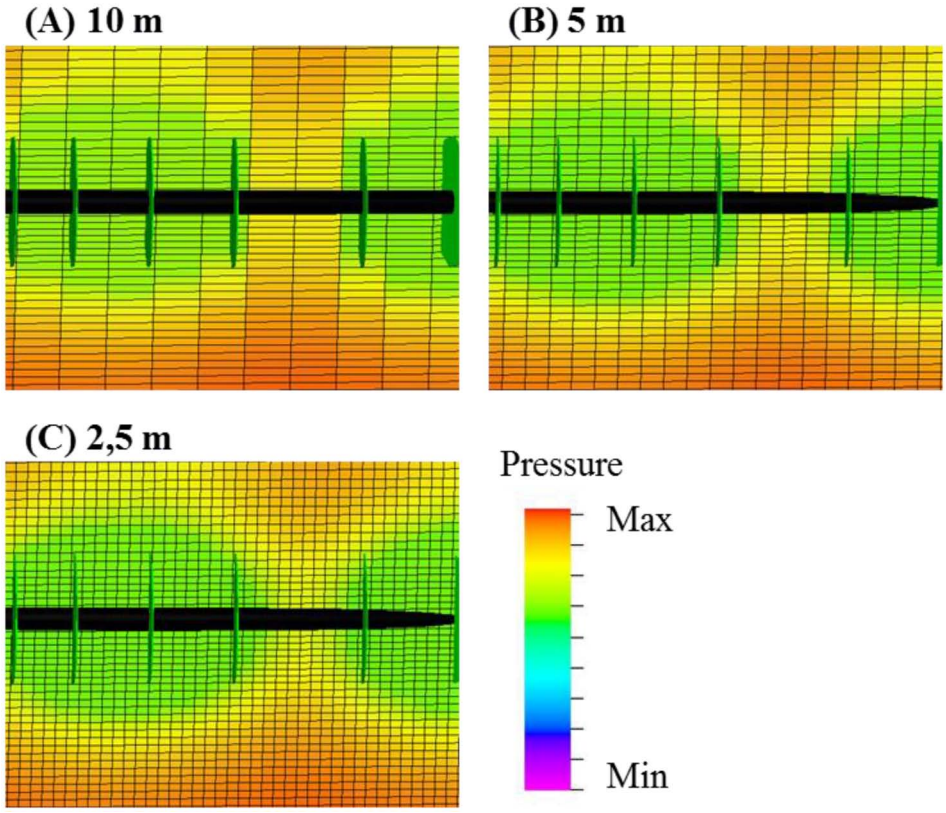

Figure 9—Different pressure cross sections with three different cell sizes in a simulation of a horizontal well. The perforations are shown in green, and the cells in the background show the pressure in the matrix around the fractured region.

Rock Compaction Model

We have matrix pore volume compressibility lab measurements available from Vaca Muerta rock samples showing that it is dependent on lithology. However, we use an average for the simulation considering that this compaction can be neglected compared to fracture compressibility.

Rock compressibility (c_f) is defined as the change rate of pore volume (V_p) with respect to pore pressure (p), divided the pore volume, this is:

$$c_f = \frac{1}{V_p}\frac{dV_p}{dp}$$

If we assume a constant value for the pore volume compressibility, we obtain the expression of pore volume as a function of pore pressure:

$$V_p(p) = V_p^0 e^{\overline{c_f}(p-p_0)}$$

In the dual porosity model we use two different compressibility tables, one for the matrix and another for the fracture.

Fracture transmissibility reduction, as we have seen, is a key mechanism to explain the production behavior. This effect is the result of complex mechanisms such as proppant crashing, embedment in the formation rock and other effects (as listed by Zhou et al. 2011, Alramahi et al. 2012, Han et al. 2014). The effect of fracture transmissibility reduction has been replicated in lab experiments.

We have chosen to model the transmissibility reduction as a power of pore volume reduction with an exponent N. Then we can obtain the fracture permeability (k_f) reduction table as

$$\frac{k_f(p)}{k_f^0} = \left(\frac{V_p(p)}{V_p^0}\right)$$

After a few iterations we observed that N = 4 is required for HM. We have used the same parameter between wells, but an experimental confirmation of this value is still needed.

The model also offers the possibility to model changes of sigma with pressure, but as we cannot differentiate both effects, we chose to model all the productivity losses as transmissibility reduction.

History Match and Forecasts

During the HM process the simulation is constrained by separator pressure and choke diameter. Results are evaluated by comparing simulated and observed gas rate, WGR and BHP (calculated from THP data as mentioned above).

Initially static model and fluid properties are fixed at the best estimates and kept unchanged during HM (see Fig. 10). Fracture properties are also initially estimated on external data; however, they are modified in each iteration until a HM is achieved. The result is a set of parameters which defines a history-matched scenario that can be used to run forecasts. The process and variables involved are shown in Fig. 10.

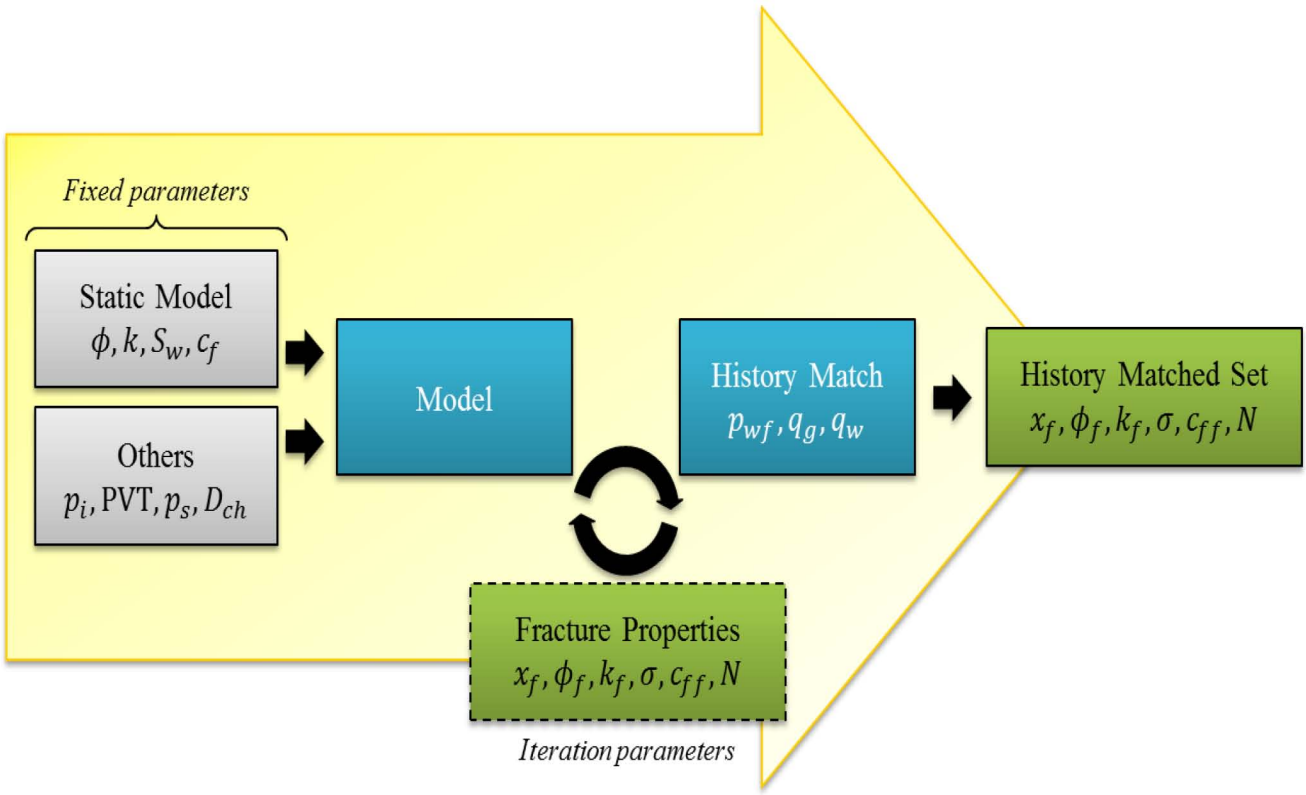

Figure 10—The HM process flowchart, showing input parameters in gray, and iteration parameters in green. The HM is considered acceptable when the BHP and rates are similar to observed data. At this point the parameters set are considered matched.

Since both the rock and fluid properties are uncertain, and we know that the HM is not unique, we define different scenarios varying these properties. Each of these scenarios goes into the process described above resulting in its own set of fracture parameters.

Finally, we obtain a set of history-matched models that give a range of forecasts that can be used to optimize development and aid the decision making process (Fig. 11).

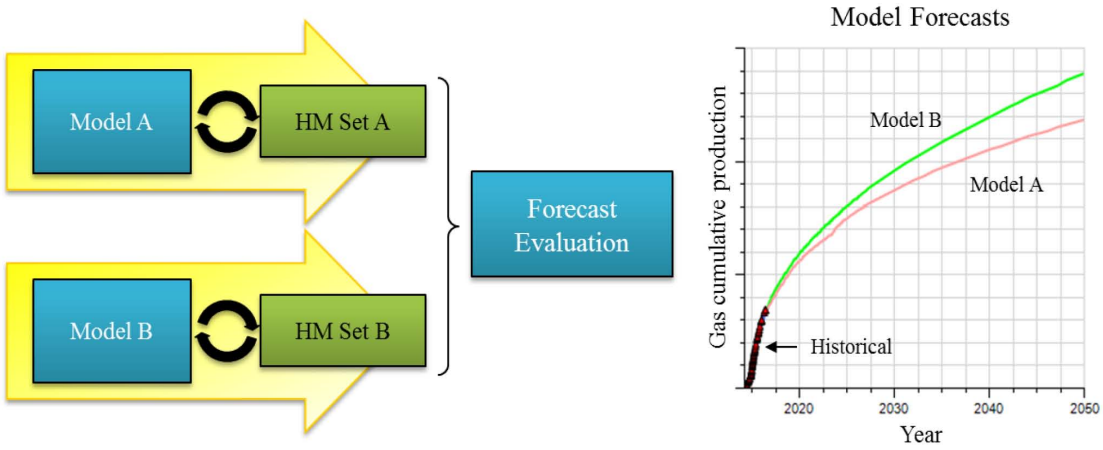

Figure 11—After a HM is conducted in each defined scenario, the forecast is used into the uncertainty analysis.

The identification of the different fracture parameters obtained by HM is useful to predict expected EUR ranges for new wells. Also this methodology is useful to compare different landing points or completion strategies, showing what EUR range can be expected with the static and fracture parameters that have been HM to date.

Simulation results for a typical well model are shown in Fig. 12. Model construction and HM process took two weeks, with an average simulation runtime of 30 minutes.

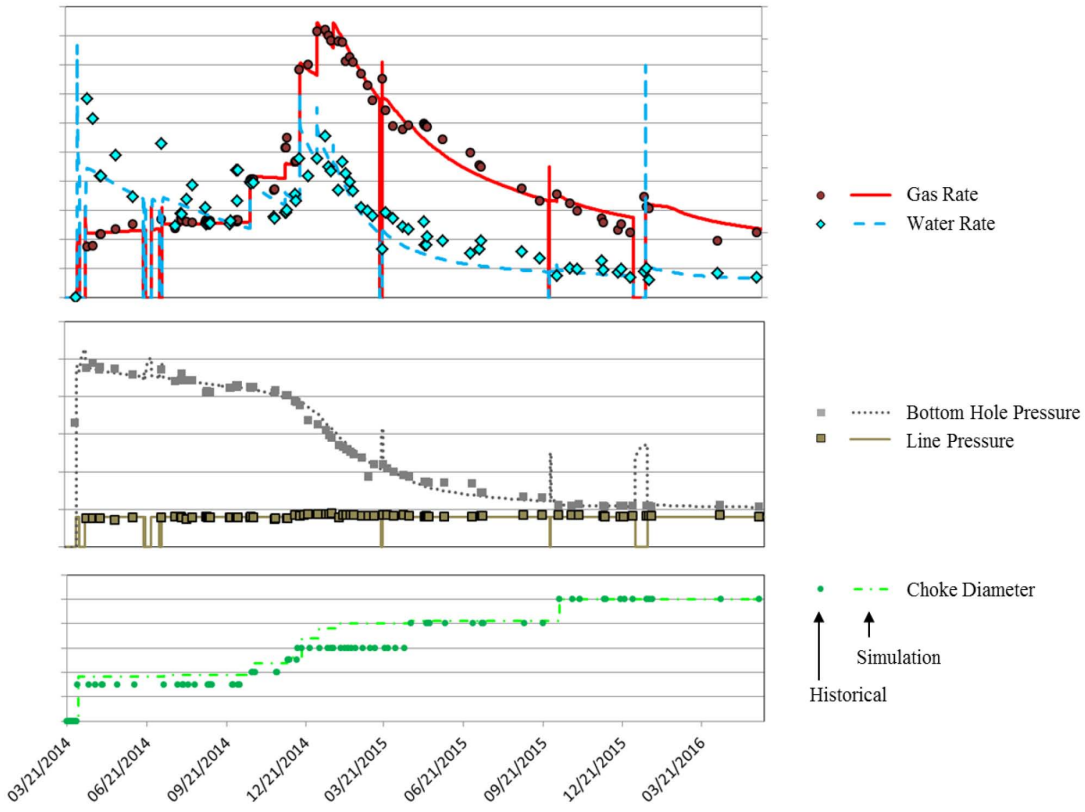

Figure 12—Simulation and historical data of a sample well including gas and water rates, BHP, line pressure and choke changes.

Conclusions

The following conclusions resulted from this study:

1. Hydraulic fractures can be represented by a dual porosity model confined in the stimulated volume around the perforations. Some of the fracture properties will be dependent on the existing natural fracture network but also on the conducted stimulation.
2. The fracture properties in the model can be inherited from a DFN or fracture geometry data, but they will be HM parameters because of their high degree of uncertainty. However, these parameters should show consistency between wells drilled and stimulated in similar conditions. If this is demonstrated, extrapolation to new wells will be more robust.
3. Fracture compaction is a critical mechanism affecting well productivity so it is included in the simulator as a reduction in pore volume and transmissibility as a function of pressure depletion.
4. The dynamic simulation of pressure drops along the wellbore segments enabled us to observe and/or predict water holdup problems. This methodology can then focus on the impact of the model variables on well productivity regardless of whether these problems occur or not.
5. Using separator/line pressure to constrain the model gives us predictability of the wells behavior under different production regimes. This allows different production strategies to be evaluated.
6. Dual porosity models can be built for one or two wells with high resolution grids running in short simulation times (between 15 minutes and 1 hour), being a flexible methodology to conduct multiple HM processes

Acknowledgments

Thanks YPF and Subsurface Manager Jose Luis Massaferro for allowing and encouraging this work.

Abbreviations

a_V	Area per volume unit
c_f	Formation pore volume compressibility $c_f = (1/V_p)(dV_p/dp)$
c_{ff}	Fracture pore volume compressibility
CGR	Condensate-gas ratio
d	Average length of the matrix blocks in the dual porosity model
d_x, d_y, d_z	Length of the matrix blocks in the directions x, y and z in the dual porosity model
D_{ch}	Choke diameter
e	Fracture thickness
HM	History match
k	Matrix permeability
k_f	Fracture permeability in the dual porosity model
k_f^0	Fracture permeability at reference pressure
N	Exponent for the fracture transmissibility reduction $k_{\mathrm{f}}(\mathrm{p})/k_{\mathrm{f}}^0 = \left[\mathrm{V_p}(\mathrm{p})/V_p^0\right]^N$
p	Pressure
p_0	Reference pressure
p_i	Initial pore pressure
p_l	Line pressure
p_{Res}	Reservoir pore pressure
p_s	Separator pressure
p_{wf}	Well flowing pressure (BHP)
p_{wh}	Wellhead pressure (THP)

q_g Gas production rate
S_w Water saturation
V_b Bulk volume
V_f Volume occupied by the fractures
V_m Volume occupied by the matrix
V_p Pore volume
V_p^0 Pore volume at reference pressure
V_{pf} Pore volume in the secondary porosity (inside the fractures)
WGR Water-gas ratio
x_f Fracture half-length
ϕ Matrix porosity
ϕ_f Fracture porosity in the dual porosity model $\phi_f = V_{pf}/V_b$
ϕ_p Proppant porosity inside the fractures $\phi_p = V_{pf}/V_f$
σ Matrix-fracture coupling factor

References

Alramahi, B. and Sundberg, M. I. 2012. Proppant Embedment And Conductivity of Hydraulic Fractures In Shales. 46th U.S. Rock Mechanics/Geomechanics Symposium, 24-27 June, Chicago, Illinois. ARMA-2012-291.

Beggs, H. D. and Brill, J. P. 1973. A Study of Two-Phase Flow in Inclined Pipes. *J Pet Technol* **25** (5): 607-617. SPE-4007-PA. http://dx.doi.org/10.2118/4007-PA

Collins, P. W., Badessich, M. F. and Ilk, D. 2015. Addressing Forecasting Non-Uniqueness and Uncertainty in Unconventional Reservoir Systems Using Experimental Design. Annual Technical Conference and Exhibition, 28-30 September, Houston, Texas, USA. SPE-175139-MS. http://dx.doi.org/10.2118/175139-MS

Cipolla, C. and Wallace, J. 2014. Stimulated Reservoir Volume: A Misapplied Concept?. SPE Hydraulic Fracturing Technology Conference, 4-6 February, The Woodlands, Texas, USA. SPE-168596-MS. http://dx.doi.org/10.2118/168596-MS

Dershowitz, B., LaPointe, P., Eiben, T. et al. 2000. Integration of Discrete Feature Network Methods With Conventional Simulator Approaches. *SPE Res Eval & Eng* **3** (2): 165-170. SPE-62498-PA. http://dx.doi.org/10.2118/62498-PA

Du, C., Zhan, L., Li, J. et al. 2011. Generalization of Dual-Porosity-System Representation and Reservoir Simulation of Hydraulic Fracturing-Stimulated Shale Gas Reservoirs. SPE Annual Technical Conference and Exhibition, 30 October-2 November, Denver, Colorado, USA. SPE-146534-MS. http://dx.doi.org/10.2118/146534-MS

Du, C. and Li, J. 2011. Generalization of Dual-Porosity System Representation for Hydraulic Fracturing-Stimulated Shale Reservoir (Part 2): Modeling, Simulation Workflow, and History Matching Studies. SPE Asia Pacific Oil and Gas Conference and Exhibition, 20-22 September, Jakarta, Indonesia. SPE-145752-MS. http://dx.doi.org/10.2118/145752-MS

Fuentes-Cruz, G. and Valkó, P., 2015. Revisiting the Dual-Porosity/Dual-Permeability Modeling of Unconventional Reservoir: The Induced-Interporosity Flow Field. *SPE J.* **20** (1): 124–141. SPE-173895-PA. http://dx.doi.org/10.2118/173895-PA

Gray, H. (1974). Vertical Flow Correlation in Gas Wells. User's Manual for API 14B, Subsurface Controlled Safety Valve Sizing Computer Program, Appendix B. API.

Han, J., and Wang, J. Y. (2014). Fracture Conductivity Decrease Due to Proppant Deformation and Crushing, a Parametrical Study. SPE Eastern Regional Meeting, 21-23 October, Charleston, WV, USA. SPE-171019-MS. http://dx.doi.org/10.2118/171019-MS

Holmes, J. B., Barkve, T. and Lund O. 1998. Application of a Multisegment Well Model to Simulate Flow in Advanced Wells. European Petroleum Conference, 20-22 October, The Hague, Netherlands. SPE-50646-MS. http://dx.doi.org/10.2118/50646-MS

Kazemi, H., Merril, L. S., Porterfield, K. L. et al. 1976. Numerical Simulation of Water-Oil Flow in Naturally Fracture Reservoirs. SPE J. **16** (6): 317–326. SPE-5719-PA. http://dx.doi.org/10.2118/5719-PA

Monti, L., Suarez, M., Thompson, A. et al. 2013. Modeling Vertical Multifractured Wells in Vaca Muerta Shale Oil Play, Argentina. SPE Unconventional Resources Conference, 10-12 April, The Woodlands, Texas, USA. SPE-164537-MS. http://dx.doi.org/10.2118/164537-MS

Oda, M. 1985. Permeability tensor for discontinuous rock masses. *Géotechnique* **35** (4): 483–495. http://dx.doi.org/10.1680/geot.1985.35.4.483

Perkins, T. 1993. Critical and Subcritical Flow of Multiphase Mixtures Through Chokes. SPE Drill & Compl **8** (4): 271–276. SPE-20633-PA. http://dx.doi.org/10.2118/20633-PA

Reijenstein, H., Lipinski, C., Fantin, M. et al. 2015. Where is the Vaca Muerta Sweet Spot? The Importance of Regional Facies Trends, Thickness, and Maturity in Generating Play Concepts. SPE Unconventional Resources Conference, 20-22 July, San Antonio, Texas, USA, SPE-178702/URTeC 2174109. http://dx.doi.org/10.15530/URTEC-2015-2174109

Russell D. G., Goodrich, J. H., Perry G. E. et al. 1966. Methods for Predicting Gas Well Performance. *J Pet Technol* **18** (1): 99–108. SPE-1242-PA. http://dx.doi.org/10.2118/1242-PA

Sagasti, G., Ortiz, A., Hryb, D. et al. 2014. Understanding Geological Heterogeneirty to Customize Field Development: An Example From the Vaca Muerta Unconventional Play, Argentina. Unconventional Resources Technology Conference, 25-27 August, Denver, Colorado, USA. URTeC 1923357. http://dx.doi.org/10.15530/URTEC-2014-1923357

Suarez, M., Pichon, S., Lacentre, P. et al. 2015. Fracturing-to-Production Simulation Approach for Completion Optimization in the Vaca Muerta Shale. SPE Latin American and Caribbean Petroleum Engineering Conference, 18-20 November, Quito, Ecuador. SPE-177058-MS. http://dx.doi.org/10.2118/177058-MS

Suarez, M. and Pichon, S. 2016. Combining Hydraulic Fracturing Considerations and Well Spacing Optimization for Pad Development in the Vaca Muerta Shale. Unconventional Resources Technology Conference, 1-3 August, San Antonio, Texas, USA. URTeC 2436107.

Warren, J. E. and Root, P. J. 1963. The Behavior of Naturally Fractured Reservoirs. *SPE J*. **3** (3): 245–255. SPE-426-PA. http://dx.doi.org/10.2118/426-PA

Weng, X., Kresse, O., Coen, C. et al. 2011. Modeling of Hydraulic-Fracture-Network Propagation in a Naturally Fractured Formation. *SPE Prod & Oper* **26** (4): 368–380. SPE-140253-PA. http://dx.doi.org/10.2118/140253-PA

Zhou, D., Zhang, G., Ruan, M., et al. 2011. Comparison of Fracture Conductivities from Field and Lab. International Petroleum Technology Conference. International Petroleum Technology Conference, 15-17 November, Bangkok, Thailand. IPTC-14706-MS. http://dx.doi.org/10.2523/IPTC-14706-MS

Appendix A

Geometrical relationship of dual porosity model parameters

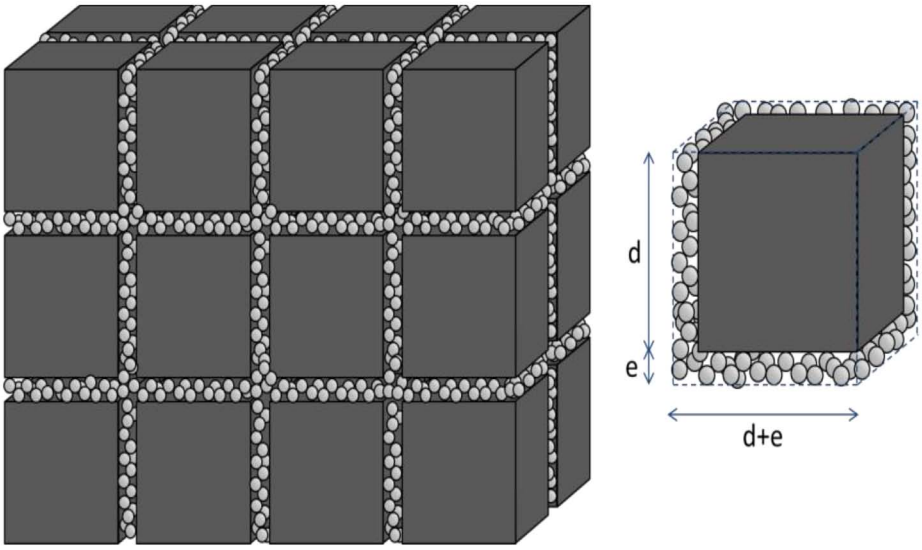

Figure 13—Scheme of the geometry implicit in the dual porosity model, showing the characteristic distances.

Kazemi explains that for 3 fracture sets,

$$\sigma = 4\left(\frac{1}{d_x^2}+\frac{1}{d_y^2}+\frac{1}{d_z^2}\right)$$

Fig. 13 shows the conceptual model of the fractured dual porosity media in which $d_x=d_y=d_z=d$ then

$$\sigma = \frac{12}{d^2}$$
$$d = \sqrt{12/\sigma}$$

Also, for a representative element (see Fig. 13), the bulk volume is

$$V_b = (d+e)^3$$

The fracture volume inside the element is the bulk volume minus the matrix volume d^3:

$$V_f = V_b - V_m = (d+e)^3 - d^3$$

As the fractures are filled with the proppant, the (secondary) pore volume is:

$$V_{pf} = \phi_p V_f = \phi_p[(d+e)^3 - d^3]$$

Then, the secondary porosity, related to the bulk volume, is:

$$\phi_f = \frac{V_{pf}}{V_b} = \phi_p \frac{(d+e)^3 - d^3}{(d+e)^3}$$

The area of contact between matrix and fracture in the element is $6d^2$, then the area per volume unit is (assuming when $e \ll d$, we can use $d+e \approx d$):

$$a_V = \frac{6d^2}{(d+e)^3} \cong \frac{6}{d} = \frac{6}{\sqrt{12}}\sqrt{\sigma} = \sqrt{3\sigma}$$